



Versatile two-dimensional boron monosulfide polymorphs with tunable bandgaps and superconducting properties

Cite as: Appl. Phys. Lett. **117**, 013103 (2020); <https://doi.org/10.1063/5.0006059>

Submitted: 28 February 2020 . Accepted: 20 June 2020 . Published Online: 06 July 2020

Dong Fan , Shaohua Lu, Chengke Chen, Meiyang Jiang, Xiao Li, and Xiaojun Hu 



View Online



Export Citation



CrossMark

Lock-in Amplifiers
up to 600 MHz



Versatile two-dimensional boron monosulfide polymorphs with tunable bandgaps and superconducting properties

Cite as: Appl. Phys. Lett. **117**, 013103 (2020); doi: [10.1063/5.0006059](https://doi.org/10.1063/5.0006059)

Submitted: 28 February 2020 · Accepted: 20 June 2020 ·

Published Online: 6 July 2020





View Online



Export Citation



CrossMark

Dong Fan,  Shaohua Lu, Chengke Chen, Meiyan Jiang, Xiao Li, and Xiaojun Hu^{a)} 

AFFILIATIONS

College of Materials Science and Engineering, Zhejiang University of Technology, Hangzhou 310014, China

^{a)} Author to whom correspondence should be addressed: huxj@zjut.edu.cn

ABSTRACT

The typical two-dimensional semiconductors, group IIIA chalcogenides, have garnered tremendous interest for their outstanding electronic, mechanical, and chemical properties. However, so far, there have been rare reports on boron monosulfides (BS) binary material. Here, four two-dimensional BS sheets, namely, the α -, β -, γ -, and δ -BS sheets, are proposed and discussed from first principles calculations. State-of-the-art calculations reveal all these structures are thermally and dynamically stable, indicating the potential for experimental synthesis. Specifically, for α -BS, it has a calculated exfoliation energy of 0.96 J m^{-2} , suggesting that the preparation of α -BS is feasible by the exfoliation of bulk rhombohedral-BS. Our results show that α -, β -, and γ -BS are semiconductors, whereas δ -BS is a metallic system. Remarkably, our calculations indicate that δ -BS is a superconductor with a large electron-phonon coupling ($\lambda \approx 1.51$), leading to a high superconducting critical temperature ($T_c \approx 21.56 \text{ K}$), which is the interesting property with intrinsic superconducting among all two-dimensional group IIIA chalcogenides. The potential of semiconducting BS monolayers as the gas-sensor or thermoelectric materials is also demonstrated.

Published under license by AIP Publishing. <https://doi.org/10.1063/5.0006059>

The family of two-dimensional (2D) crystals, 2D group IIIA chalcogenides, are promising materials for photoelectronics,¹ gas sensing,² and Li-ion battery anodes.³ Until now, various layered group IIIA chalcogenides, i.e., GaS,¹ GaSe,⁴ GaTe,^{5,6} and InSe,⁷ have been synthesized experimentally. Following by these achievements, great endeavors have also been made to investigate the intriguing physical and chemical properties of these materials for potential applications in many fields.^{1,2} In fact, the bulk boron-sulfur binary material is also a light-element member of group IIIA chalcogenides family. Experimentally, boron-sulfur binary compounds have been known since 1977,^{8,9} and its monosulfide structure was reported in 2001,¹⁰ namely, bulk rhombohedral boron monosulfide (r -BS). However, unlike other common group IIIA chalcogenide semiconductors, little research has been done toward preparation of the 2D binary BS compounds due to the lack of knowledge of their physical properties.^{11,12} To date, only few structural and electronic properties of bulk binary BS compounds have been reported, showing that the bulk r -BS is a semiconductor with an estimated bandgap of 3.4 eV .^{10,11} However, little research has been done toward the preparation of 2D binary BS compounds due to the lack of knowledge of their physical properties.

In this Letter, we present four BS monolayers, namely, α -, β -, γ -, and δ -BS, predicted via combined first principles calculations and structure search method. Both dynamical and thermal stabilities of these sheets are investigated by phonon spectrum calculation and *abinitio* molecular dynamics (AIMD) simulation. The electronic structure calculations show that α -, β -, and γ -BS are semiconductors with the bandgaps of 4.03, 3.89, and 2.94 eV, respectively, whereas δ -BS is a metallic sheet. Quantum transport simulations show the high molecular sensitivity of the hypothetical chemical sensing device based on α - and β -BS monolayers. More importantly, electron-phonon coupling calculations show that δ -BS is superconducting with a high superconducting critical temperature (T_c) of 21.56 K.

The search of stable BS systems is performed by using the CALYPSO package.^{13–15} All the calculations were carried out with the Vienna *Abinitio* Simulation Package.¹⁶ The density functional theory (DFT) with the generalized gradient approximation (GGA) of Perdew-Burke-Ernzerhof (PBE) functional was employed.^{17,18} Quantum-ESPRESSO 6.1 package¹⁹ is used to study the electron-phonon coupling (EPC) in δ -BS. Quantum transport simulations were performed by using the density functional theory and nonequilibrium Green's function (NEGF) method as implemented in the

QuantumATK package.²⁰ More details on computational methods can be found in the [supplementary material](#).

Optimized structures of all predicated BS sheets are shown in [Fig. 1](#), and the calculated lattice parameters are summarized in Table S1. We identify four different phases, denoted by α -, β -, γ -, and δ -BS, as shown in [Figs. 1\(a\)–1\(d\)](#), respectively. Evidently, α - and β -BS sheets share similar structural features with the experimentally fabricated 2D hexagonal GaS and GaSe.^{21,22} They adopt the hexagonal lattices with two B and two S atoms in each unit cell. The optimized lattice constants for α - and β -BS are $a = b = 3.06 \text{ \AA}$ and $a = b = 3.04 \text{ \AA}$, with space group $P-3m1$ and $P-6m2$, respectively. Also, the obtained results for β -BS are in good agreement with the previous theoretical work.¹¹ [Figure S1](#) presents the energy profile relative to the α -BS. Obviously, α -BS is energetically more stable than the β -BS (12.50 meV per formula) with an energy barrier of 0.47 eV per formula.

Interestingly, the hitherto unknown configurations, γ - and δ -BS, crystallize in the monoclinic and orthorhombic lattice with space group $C2/m$ and $Pmma$, showing the C_{2h} and D_{2h} symmetry, respectively. As shown in [Figs. 1\(c\)](#) and [1\(d\)](#), one unit cell of γ -BS (δ -BS) monolayer consists of 4 (2) B atoms and 4 (2) S atoms with the optimized lattice parameters being $a = 7.38$ (3.07) \AA and $b = 3.06$ (2.59) \AA , respectively. For δ -BS, S-B bonds play an important role and each S atom is bonded to two adjacent B atoms along the a direction. Along the b direction, S atoms line both sides of the zigzag B chains.

To examine the relative stability of these different allotropes, the cohesive energy (E_c) per atom with respect to the energy of isolated B and S atoms is calculated as defined by $E_{coh} = (nE_B + mE_S - E_{BS}) / (n + m)$, in which E_B , E_S , and E_{BS} are the calculated total energies of a single B atom, a single S atom, and the BS sheet, respectively; n (m) is the number of B(S) atoms in the unit cell. According to our calculations, these monolayers have the cohesive energies of 5.23, 5.22, 5.11, and 4.92 eV per atom for α -, β -, γ -, and δ -BS, respectively. Thus, α -BS is the energetically most stable phase, while β -, γ -, and δ -BS are the metastable phases. As a reference, the cohesive energies of the experimentally realized 2D silicene and phosphorene are 3.71 and 3.61 eV per atom, respectively.²³ Therefore, the even higher cohesive energies

can ensure that the proposed monolayers are strongly bonded with the unique chemical bonding.

The dynamical stability of these monolayers can be further checked by phonon dispersion curves as shown in [Figs. 1\(e\)](#) and [1\(f\)](#). No imaginary phonon frequencies were observed in the whole Brillouin zone, suggesting their dynamical stability. The highest frequency of γ -BS reaches up to 1073 cm^{-1} , higher than that of 473 cm^{-1} in MoS_2 ,²⁴ $t\text{-SiC}$ (735 cm^{-1}),²⁵ and silicene (580 cm^{-1}),²⁶ indicating the strong B–S and B–B bonds in the structures. Additionally, their thermal stability is also confirmed by performing the AIMD simulations, as shown in [Figs. S2](#) and [S3](#). Therefore, the above-mentioned results demonstrate that all these monolayers have satisfactory energetic, dynamical, and thermal stability. Conventionally, for a mechanically stable 2D free-standing configuration, the calculated elastic constants should satisfy $C_{11}C_{22} - C_{12}C_{21} > 0$ and $C_{66} > 0$.^{27,28} As listed in Table S1, all the calculated elastic constants of the proposed structures satisfy the criteria, indicating that these 2D compounds have favorable mechanical stability. Simultaneously, the in-plane Young's modulus (or in-plane stiffness) is calculated to be $212 \text{ GPa} \cdot \text{nm}$ for β -BS, which is distinctly higher than that of experimentally synthesized 2D GaS ($73 \text{ GPa} \cdot \text{nm}$) and silicene ($61 \text{ GPa} \cdot \text{nm}$).^{11,29} However, for γ - and δ -BS sheets, as elastic constant C_{11} is not equal to C_{22} , they are mechanically anisotropic.

The desirable mechanical properties are indispensable for applications in the real world. Besides in-plane Young's modulus, ideal strength is also an important mechanical property for 2D material.³⁰ The ideal tensile stress vs strain for the BS sheets is shown in [Fig. S4](#). With small strains deformations, the sheets exhibit linear stress-strain relationship (with distinguished elastic anisotropy for γ - and δ -BS). As the applied strain increases, their stress-strain behaviors become nonlinear and show difference, changing trends along the x and y directions. Particularly, for α - and β -BS, along the y direction, both the peak strengths and the corresponding critical strains are higher than along the x direction, while the opposite trends occurred in γ - and δ -BS sheets. α -BS can sustain stress up to 13 N m^{-1} and 18 N m^{-1} in the x and y directions, respectively. The corresponding critical strains are 0.1 (x) and 0.22 (y). The ideal strengths for the β -BS are 16 N m^{-1} and 20 N m^{-1} in the x and y directions, respectively, and their critical strains are 0.12 (x) and 0.24 (y). For δ -BS, its peak strength is 25 N m^{-1} at $\epsilon_x = 0.34$ and 6 N m^{-1} at $\epsilon_y = 0.06$, respectively. Thus, the ideal strengths of BS sheets are significantly higher than other 2D materials, such as borophene, MoS_2 , and phosphorene.³⁰

The computed HSE06 band structures of the proposed sheets are shown in [Fig. 2](#). For α - and β -BS, clearly, they are indirect bandgap semiconductors: the conduction band minimum (CBM) is at the M point, while the valence band maximum (VBM) lies between the Γ and K points, which is only slightly higher in energy than at the Γ point (6.6 meV for α -BS and 16.2 meV for β -BS at HSE06 level). However, for γ -BS, both CBM and VBM are located at the Γ point, generating a direct bandgap of 2.94 eV. For those three semiconductors, their band structures show strong anisotropy of the conduction band, which finally leads to the anisotropy of the effective masses as shown in [Fig. S5](#).

Interestingly, the top valence bands of α - and β -BS sheets are nearly flat near around the Γ point, leading to the Mexican-hat shape of valence band edges, which render sharp peaks in the DOS and strong van Hove singularities near the Fermi level.^{31–33}

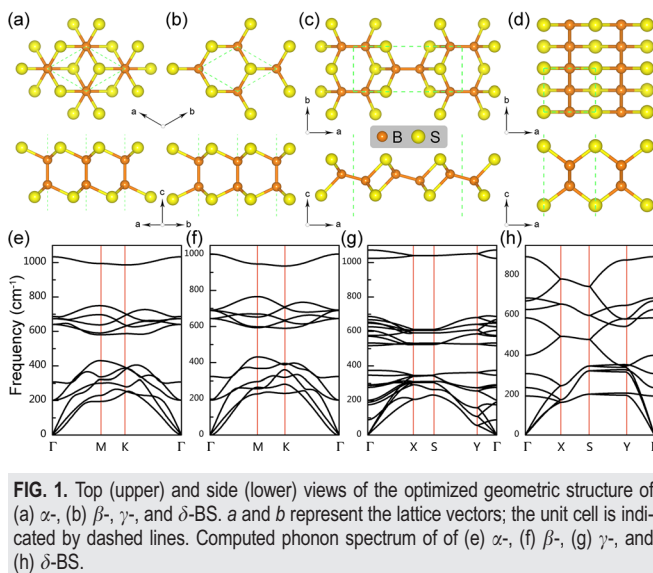


FIG. 1. Top (upper) and side (lower) views of the optimized geometric structure of (a) α -, (b) β -, γ -, and δ -BS. a and b represent the lattice vectors; the unit cell is indicated by dashed lines. Computed phonon spectrum of (e) α -, (f) β -, (g) γ -, and (h) δ -BS.

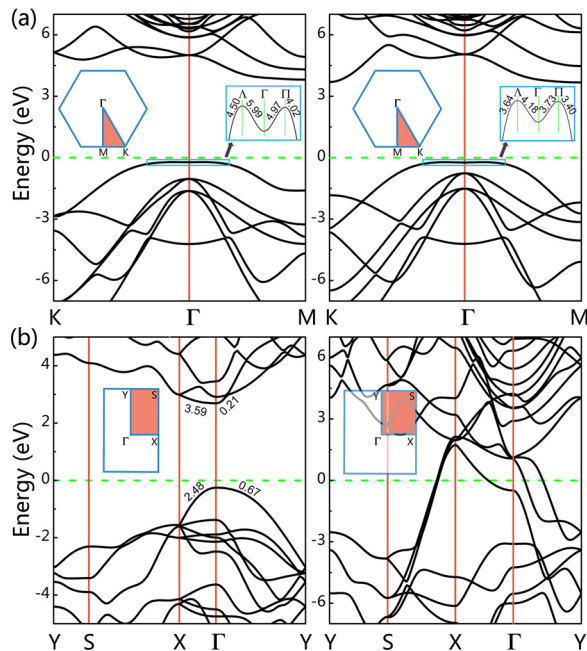


FIG. 2. Electronic band structures for (a) α - (left), β - (right), (b) γ - (left), and δ -BS (right) at HSE06 level. The Fermi energy level is set to zero. The corresponding high symmetry points in the first Brillouin-Zone and the effective electron and hole masses (GGA-PBE) are also inserted.

The Mexican-hat shape valence bands are mostly contributed by the $2p$ and $2p$ orbitals of B and S atoms, respectively, and these orbitals are strongly overlapping in the full energy range, suggesting covalent bonding characters of B-S bonds (see Fig. S6). The covalent features in the proposed 2D materials are also demonstrated by the analysis of the electron localization functions (ELFs) as shown in Fig. S7. Obviously, ELFs show two localization areas: one is located around the B-S bonds and the other is between B-B bonds, reflecting the valence electrons are shared between the adjacent atoms.

To evaluate the performance of monolayer BS as a gas sensor, we calculated the $I - V$ characteristics before and after the typical molecular adsorption, using the NEGF formalism coupled with the density functional theory calculations. For the cost of computation, we only consider two energy-favorable structures: α - and β -BS. Quantum transport calculations were carried out for α - and β -BS with some molecular adsorption, including H_2O , CO_2 , and NH_3 . The most stable adsorbed configurations for the adsorption of different gas molecules on α - and β -BS sheets are considered. The simulated $I - V$ curves are shown in Fig. 3.

One can see that the current changes significantly upon adsorption of the NH_3 and H_2O molecule, in both α - and β -BS, suggesting the high sensitivity of this sensing device. Relative to the CO_2 adsorption, we found that the sensitivity of α -BS toward H_2O adsorption decreases by 51% when the applied bias voltage is 1.0 V. Thus, the transport features of α - and β -BS monolayers exhibit apparent responses with the striking change of $I - V$ relationship before and after H_2O or NH_3 adsorption.

One of the promising avenues to tune the electronic property of 2D materials is strain engineering. The bandgaps of α -, β -, and γ -BS

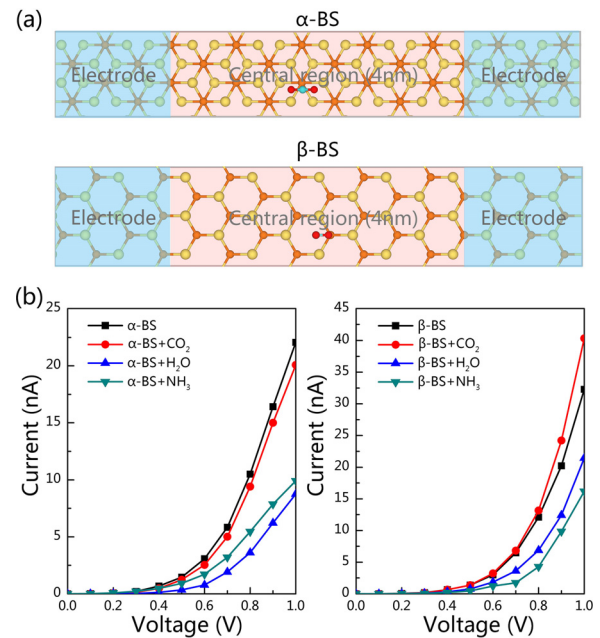


FIG. 3. (a) A schematic illustration of α - and β -BS-based sensor for detecting gas molecule. In order to avoid the tunneling effect, the length of the central region was set to 4 nm. (b) The simulated $I - V$ characteristics before and after the adsorption of gas molecule on α - (left) and β -BS (right) monolayers.

structures with respect to the uniaxial stress are shown in Fig. 4(a). Approximately, the bandgaps of the α - and β -BS monolayers decrease gradually with either tensile or compressive strains, showing a non-monotonic relationship. This unusual behavior is attributed to Mexican-hat shape valence bands near the Fermi level, akin to the InP_3 monolayer.³¹ Their outstanding properties with heavy effective masses and wide bandgaps render these materials suitable candidates for future applications in ultrashort (i.e., sub-5 nm regime) channel logical devices.^{35,35}

Additionally, the metallic property of δ -BS inspires us to investigate its potential superconducting property. Figure 4(b) shows the Eliashberg spectral function $\alpha^2F(\omega)$ together with the integrated EPC parameter $\lambda(\omega)$ at the PBE level. $\alpha^2F(\omega)$ exhibits a strong peak around 5 THz, and $\lambda(\omega)$ increases sharply in the range of 0–7 THz. As expected, the main contributor to the EPC is derived from the vibration of the heavy S atoms. The resulting coupling strength of $\lambda \approx 1.51$ is rather strong. Superconducting transition temperature (T_c) of δ -BS is estimated through the Allen-Dynes modified McMillan formula equation,³⁶

$$T_c = \frac{\omega_{\log}}{1.2} \exp\left(-\frac{1.04[1 + \lambda]}{\lambda - \mu^*[1 + 0.62\lambda]}\right), \quad (1)$$

by using the calculated logarithmic average frequency (ω_{\log}) and a series of Coulomb pseudopotential parameters (μ^*) from 0.10 to 0.13 as shown in Table S2. At $\mu^* = 0.10$, the highest T_c value of δ -BS is 21.56 K, originating from its strong EPC and high logarithmic average frequency ($\omega_{\log} = 189.06$ K). Thus, the evaluated T_c is in the range of 21.56 K ($\mu^* = 0.10$) to 19.08 K ($\mu^* = 0.13$), indicating that the δ -BS is

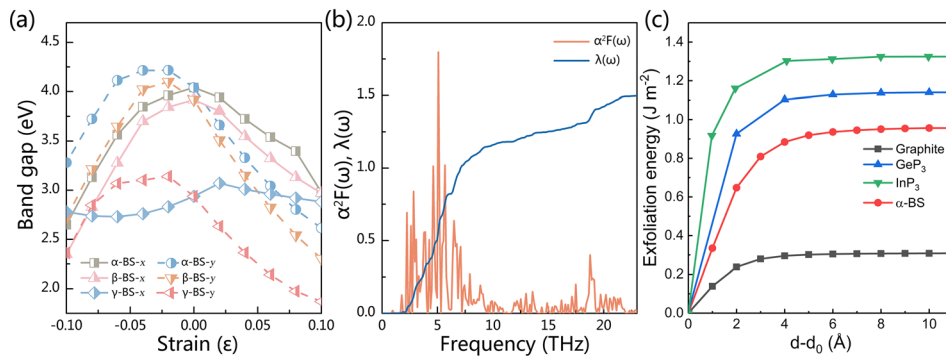


FIG. 4. (a) Dependence of the fundamental bandgap on the in-plane uniaxial strain along the x (solid lines) and y (dashed lines) directions for α -, β -, and γ -BS. (b) Calculated Eliashberg EPC spectral function and corresponding integral of the δ -BS structure. (c) Calculated exfoliation energy vs separation distance for α -BS in comparison with graphite, where d_0 indicates the van der Waals (with vdW-DF correction³⁴) gap between adjacent layers in bulk r -BS crystal.

an intrinsic Bardeen–Cooper–Schrieffer (BCS) type superconductor. Notably, this T_c is higher than that of other previously reported 2D superconductors, such as borophenes (≈ 10 – 20 K) and boron carbides (≈ 21.20 K).^{37,38}

The most common techniques to prepare 2D materials from their bulk counterparts are mechanical or liquid phase exfoliation.^{39,40} Here, to explore the possibility of fabricating the energetically favorable α -BS from the surface of its layered bulk r -BS crystal (see Fig. S7),^{10,41} we then simulated the exfoliation process and calculated exfoliation energy with respect to separation, as shown in Fig. 4(c). We first test the computing method using graphite as a benchmark and the calculated exfoliation energy for graphene is 0.30 J m^{-2} , which is consistent with the previous experimental ($0.32 \pm 0.03 \text{ J m}^{-2}$)⁴² and theoretical value (0.31 J m^{-2}).³¹ For α -BS, the calculated exfoliation energy is 0.96 J m^{-2} , which is higher than that of graphene, but still less than some layered materials, i.e., InP_3 (1.32 J m^{-2}),³¹ Ca_2N (1.08 J m^{-2}),⁴³ and GeP_3 (1.14 J m^{-2}),⁴⁴ indicating the α -BS sheet could be prepared experimentally from its bulk counterpart. Therefore, the moderate vdW interactions of α -BS suggest the preparation of mono- or few-layer α -BS heterostructures is feasible.⁴⁵

In summary, we have reported four 2D BS binary sheets with high stability, high mechanical strength, and unique electronic properties. Importantly, δ -BS phase is identified as the discovery of intrinsic superconducting material among all 2D group IIIA chalcogenides. All monolayers show good dynamical and thermal stability, and α -BS is expected to be prepared from its layered bulk r -BS by exfoliation. The quantum transport features of α - and β -BS monolayers exhibit distinct responses with a change of I – V relationship before and after H_2O (NH_3) adsorption. Therefore, we predict that α - and β -BS monolayers could be promising candidates for the gas sensor with high sensitivity. These advantaged features promote 2D BS sheets as promising candidates for future applications in future nano-devices. We also believe our results will further stimulate the experimental preparation and investigation of 2D BS materials.

See the [supplementary material](#) for computational details, lattice parameters, electron–phonon coupling parameter, fluctuations of the total energy, band structures at GGA–PBE level, partial density of states, and location function of α -, β -, γ -, and δ -BS monolayers.

AUTHORS' CONTRIBUTIONS

X. Hu and D. Fan designed the research. D. Fan carried out the systematic structure search, *ab initio* calculations, and interpreted the

data. D. Fan wrote the manuscript with the support from S. Lu, C. Chen, X. Li, and M. Jiang. X. Hu coordinated the research.

The work was performed at the National Supercomputer Center in Guangzhou, and the calculations were carried out on TianHe-2. This work was supported by the Key Project of the National Natural Science Foundation of China (No. U1809210), the National Natural Science Foundation of China (Nos. 11504325, 50972129, and 50602039), and the National Science Foundation of Zhejiang Province (No. LQ15A040004). It was also supported by the International Science Technology Cooperation Program of China (No. 2014DFR51160), the National Key Research and Development Program of China (No. 2016YFE0133200), the One Belt and One Road International Cooperation Project from Key Research and Development Program of Zhejiang Province (No. 2018C04021), and the European Union's Horizon 2020 Research and Innovation Staff Exchange (RISE) Scheme (No. 734578).

DATA AVAILABILITY

The data that support the findings of this study are available within the article and the [supplementary material](#). The structural data in this work and the output of the NVT-MD simulation results that support the findings of this study are also available at <https://github.com/agrh/Papers>.

REFERENCES

- P. Hu, L. Wang, M. Yoon, J. Zhang, W. Feng, X. Wang, Z. Wen, J. C. Idrobo, Y. Miyamoto, and D. B. Geohegan, "Highly responsive ultrathin gas nanosheet photodetectors on rigid and flexible substrates," *Nano Lett.* **13**, 1649–1654 (2013).
- S. Yang, Y. Li, X. Wang, N. Huo, J.-B. Xia, S.-S. Li, and J. Li, "High performance few-layer gas photodetector and its unique photo-response in different gas environments," *Nanoscale* **6**, 2582–2587 (2014).
- S. Yu, Y.-C. Rao, S.-F. Li, and X.-M. Duan, "Net W monolayer: A high-performance electrode material for Li-ion batteries," *Appl. Phys. Lett.* **112**, 053903 (2018).
- K. Cheng, Y. Guo, N. Han, X. Jiang, J. Zhang, R. Ahuja, Y. Su, and J. Zhao, "2D lateral heterostructures of group-III monochalcogenide: Potential photovoltaic applications," *Appl. Phys. Lett.* **112**, 143902 (2018).
- Z. Wang, K. Xu, Y. Li, X. Zhan, M. Safdar, Q. Wang, F. Wang, and J. He, "Role of Ga vacancy on a multilayer gate phototransistor," *ACS Nano* **8**, 4859–4865 (2014).
- Z. Wang, M. Safdar, M. Mirza, K. Xu, Q. Wang, Y. Huang, F. Wang, X. Zhan, and J. He, "High-performance flexible photodetectors based on gate nanosheets," *Nanoscale* **7**, 7252–7258 (2015).

- ⁷N. T. Hung, A. R. Nugraha, and R. Saito, "Two-dimensional InSe as a potential thermoelectric material," *Appl. Phys. Lett.* **111**, 092107 (2017).
- ⁸H. Diercks and B. Krebs, "Crystal structure of B₂S₃: Four-membered B₂S₂ rings and six-membered B₃S₃ rings," *Angew. Chem., Int. Ed.* **16**, 313–313 (1977).
- ⁹B. Krebs and H.-U. Hürter, "B₈S₁₆-An 'inorganic porphine,'" *Angew. Chem., Int. Ed.* **19**, 481–482 (1980).
- ¹⁰T. Sasaki, H. Takizawa, K. Uheda, and T. Endo, "High pressure synthesis of binary B–S compounds," *Phys. Status Solidi B* **223**, 29–33 (2001).
- ¹¹S. Demirci, N. Avazli, E. Durgun, and S. Cahangirov, "Structural and electronic properties of monolayer group III monochalcogenides," *Phys. Rev. B* **95**, 115409 (2017).
- ¹²B. Mortazavi and T. Rabczuk, "Boron monochalcogenides; stable and strong two-dimensional wide band-gap semiconductors," *Energies* **11**, 1573 (2018).
- ¹³Y. Wang, J. Lv, L. Zhu, and Y. Ma, "Crystal structure prediction via particle-swarm optimization," *Phys. Rev. B* **82**, 094116 (2010).
- ¹⁴Y. Wang, J. Lv, L. Zhu, and Y. Ma, "CALYPSO: A method for crystal structure prediction," *Comput. Phys. Commun.* **183**, 2063–2070 (2012).
- ¹⁵B. Gao, P. Gao, S. Lu, J. Lv, Y. Wang, and Y. Ma, "Interface structure prediction via CALYPSO method," *Sci. Bull.* **64**, 301–309 (2019).
- ¹⁶G. Kresse and J. Hafner, "Ab initio molecular dynamics for liquid metals," *Phys. Rev. B* **47**, 558 (1993).
- ¹⁷P. E. Blöchl, "Projector augmented-wave method," *Phys. Rev. B* **50**, 17953 (1994).
- ¹⁸J. P. Perdew, K. Burke, and M. Ernzerhof, "Generalized gradient approximation made simple," *Phys. Rev. Lett.* **77**, 3865 (1996).
- ¹⁹P. Giannozzi, S. Baroni, and N. Bonini, "QUANTUM ESPRESSO: A modular and open-source software project for quantum simulations of materials," *J. Phys.: Condens. Matter* **21**, 395502 (2009).
- ²⁰M. Brandbyge, J.-L. Mozos, P. Ordejón, J. Taylor, and K. Stokbro, "Density-functional method for nonequilibrium electron transport," *Phys. Rev. B* **65**, 165401 (2002).
- ²¹D. J. Late, B. Liu, J. Luo, A. Yan, H. Matte, M. Grayson, C. Rao, and V. P. Dravid, "GaS and GaSe ultrathin layer transistors," *Adv. Mater.* **24**, 3549–3554 (2012).
- ²²P. Hu, Z. Wen, L. Wang, P. Tan, and K. Xiao, "Synthesis of few-layer GaSe nanosheets for high performance photodetectors," *ACS Nano* **6**, 5988–5994 (2012).
- ²³Y. Wang, F. Li, Y. Li, and Z. Chen, "Semi-metallic Be₅C₂ monolayer global minimum with quasi-planar pentacoordinate carbons and negative Poisson's ratio," *Nat. Commun.* **7**, 11488 (2016).
- ²⁴A. Molina-Sanchez and L. Wirtz, "Phonons in single-layer and few-layer MoS₂ and WS₂," *Phys. Rev. B* **84**, 155413 (2011).
- ²⁵D. Fan, S. Lu, Y. Guo, and X. Hu, "Novel bonding patterns and optoelectronic properties of the two-dimensional sixcy monolayers," *J. Mater. Chem. C* **5**, 3561–3567 (2017).
- ²⁶S. Cahangirov, M. Topsakal, E. Aktürk, H. Şahin, and S. Ciraci, "Two- and one-dimensional honeycomb structures of silicon and germanium," *Phys. Rev. Lett.* **102**, 236804 (2009).
- ²⁷Q. Wei and X. Peng, "Superior mechanical flexibility of phosphorene and few-layer black phosphorus," *Appl. Phys. Lett.* **104**, 251915 (2014).
- ²⁸D. Fan, S. Lu, C. Chen, M. Jiang, X. Li, and X. Hu, "A novel hydrogenated boron-carbon monolayer with high stability and promising carrier mobility," *Phys. Chem. Chem. Phys.* **21**, 2572–2577 (2019).
- ²⁹H. Zhang and R. Wang, "The stability and the nonlinear elasticity of 2D hexagonal structures of Si and Ge from first-principles calculations," *Physica B* **406**, 4080–4084 (2011).
- ³⁰Z. Zhang, Y. Yang, E. S. Penev, and B. I. Yakobson, "Elasticity, flexibility, and ideal strength of borophenes," *Adv. Fun. Mater.* **27**, 1605059 (2017).
- ³¹N. Miao, B. Xu, N. C. Bristowe, J. Zhou, and Z. Sun, "Tunable magnetism and extraordinary sunlight absorbance in indium triphosphide monolayer," *J. Am. Chem. Soc.* **139**, 11125–11131 (2017).
- ³²T. Cao, Z. Li, and S. G. Louie, "Tunable magnetism and half-metallicity in hole-doped monolayer GaSe," *Phys. Rev. Lett.* **114**, 236602 (2015).
- ³³A. Kuc, T. Cusati, E. Dib, A. F. Oliveira, A. Fortunelli, G. Iannaccone, T. Heine, and G. Fiori, "High-performance 2D p-type transistors based on GaSe layers: An ab initio study," *Adv. Electron. Mater.* **3**, 1600399 (2017).
- ³⁴M. Dion, H. Rydberg, E. Schröder, D. C. Langreth, and B. I. Lundqvist, "Van der waals density functional for general geometries," *Phys. Rev. Lett.* **92**, 246401 (2004).
- ³⁵G. Fiori, F. Bonaccorso, G. Iannaccone, T. Palacios, D. Neumaier, A. Seabaugh, S. K. Banerjee, and L. Colombo, "Electronics based on two-dimensional materials," *Nat. Nanotechnol.* **9**, 768 (2014).
- ³⁶P. B. Allen and R. Dynes, "Transition temperature of strong-coupled superconductors reanalyzed," *Phys. Rev. B* **12**, 905 (1975).
- ³⁷E. S. Penev, A. Kutana, and B. I. Yakobson, "Can two-dimensional boron superconduct?," *Nano Lett.* **16**, 2522–2526 (2016).
- ³⁸D. Fan, S. Lu, Y. Guo, and X. Hu, "Two-dimensional stoichiometric boron carbides with unexpected chemical bonding and promising electronic properties," *J. Mater. Chem. C* **6**, 1651–1658 (2018).
- ³⁹K. S. Novoselov, A. K. Geim, S. V. Morozov, D. Jiang, Y. Zhang, S. V. Dubonos, I. V. Grigorieva, and A. A. Firsov, "Electric field effect in atomically thin carbon films," *Science* **306**, 666–669 (2004).
- ⁴⁰K. S. Kim, Y. Zhao, H. Jang, S. Y. Lee, J. M. Kim, K. S. Kim, J.-H. Ahn, P. Kim, J.-Y. Choi, and B. H. Hong, "Large-scale pattern growth of graphene films for stretchable transparent electrodes," *Nature* **457**, 706 (2009).
- ⁴¹K. A. Cherednichenko, I. A. Kruglov, A. R. Oganov, Y. L. Godec, M. Mezouar, and V. L. Solozhenko, "Boron monosulfide: Equation of state and pressure-induced phase transition," *J. Appl. Phys.* **123**, 135903 (2018).
- ⁴²R. Zacharia, H. Ulbricht, and T. Hertel, "Interlayer cohesive energy of graphite from thermal desorption of polyaromatic hydrocarbons," *Phys. Rev. B* **69**, 155406 (2004).
- ⁴³S. Zhao, Z. Li, and J. Yang, "Obtaining two-dimensional electron gas in free space without resorting to electron doping: An electronegative design," *J. Am. Chem. Soc.* **136**, 13313–13318 (2014).
- ⁴⁴Y. Jing, Y. Ma, Y. Li, and T. Heine, "GeP₃: A small indirect band gap 2D crystal with high carrier mobility and strong interlayer quantum confinement," *Nano Lett.* **17**, 1833–1838 (2017).
- ⁴⁵C. Tan and H. Zhang, "Epitaxial growth of hetero-nanostructures based on ultrathin two-dimensional nanosheets," *J. Am. Chem. Soc.* **137**, 12162–12174 (2015).